Journal of Power Sources 195 (2010) 4622–4627

Contents lists available at ScienceDirect

Journal of Power Sources

journal homepage: www.elsevier.com/locate/jpowsour

Effect of gas composition on Ru dissolution and crossover in polymer-electrolyte membrane fuel cells

Tommy T.H. Cheng*, Nengyou Jia, Vesna Colbow, Silvia Wessel, Monica Dutta

Ballard Power Systems, Inc., 9000 Glenlyon Parkway, Burnaby, BC V5J 5J8, Canada

ARTICLE INFO

Article history:
Received 20 January 2010
Received in revised form 10 February 2010
Accepted 11 February 2010
Available online 18 February 2010

Keywords:
PEMFC
Gas composition
Ru dissolution
Ru crossover
Catalyst degradation

ABSTRACT

Pt–Ru-based anodes are commonly used in polymer-electrolyte membrane fuel cells (PEMFCs) to provide improved CO tolerance for reformate fuel applications. However, Ru crossover from the anode to the cathode has been identified as a critical durability problem that has severe performance implications. In the present study, an anode accelerated stress test (AST) was used to simulate potential spikes that occur during fuel cell start-ups and shutdowns to induce Ru crossover. The effects of fuel gas composition, namely hydrogen and carbon dioxide concentrations, on Ru dissolution and crossover were investigated. The cell performance losses were correlated with the degree of Ru crossover as determined by the changes in cathode cyclic voltammetry (CV) characteristics and neutron activation analysis (NAA). It was found that higher hydrogen concentration in the fuel accelerated Ru crossover and that the presence of carbon dioxide hindered Ru crossover. In particular, the injection of 20 vol.% carbon dioxide during potential cycling resulted in very minor Ru crossover, which showed essentially identical performance losses and CV characteristic changes as a fuel cell composed of a Ru-free anode. The experimental results suggest that the Ru species in our Pt–Ru metal oxide catalysts need to go through a reduction step by hydrogen before dissolution. The presence of carbon dioxide may play a role in hindering the reduction step.

1. Introduction

Polymer-electrolyte membrane fuel cells (PEMFCs) are promising energy conversion devices that can operate in a wide range of applications, including light and heavy-duty vehicles, back-up power for telecom communications, and stationary cogeneration systems. One of the most critical obstacles for fuel cell commercialization is durability. The current durability targets for PEMFCs are 40,000 and 5000 h for stationary and automotive applications, respectively [1]. As a result, much research attention has shifted to improve the PEMFC durability by both fundamentally understanding the degradation mechanisms and subsequently developing more durable materials for fuel cell use. Since the last decade, studies of the different failure modes of PEMFCs have led to stronger understanding of various degradation modes of different components, including membranes, electrocatalysts, and gas diffusion layers (GDLs) [2–6]. These degradation mechanisms have been reviewed extensively by Borup et al. [7]. Owing to these efforts, much progress has been made in improving the durability, reliability, and lifetime of PEMFCs.

The electrocatalysts employed in PEMFCs are typically carbon-supported Pt nanoparticles. It is well known that catalyst degradation is caused by Pt dissolution, agglomeration, and carbon corrosion [8–10], and results in significant reduction in electrochemical active area and changes in catalyst layer hydrophobicity, leading to kinetic and mass transport losses. Moreover, catalyst contamination by SO_2, H_2S, NO_2, NH_3, and CO is also known to be detrimental to the lifetime of the PEMFC [11–15]. Due to the limitations in reforming technology to cost-effectively produce clean hydrogen, the presence of CO is normally unavoidable in reformate-based fuel cell systems. In general, CO in the fuel stream is mitigated with either the use of air bleed and/or the use of CO tolerant catalysts. However, the use of air bleed leads to higher system complexity, reduction in fuel efficiency, and membrane degradation, which in turn translates into higher system costs [16]. Furthermore, air bleed alone is typically not sufficient to minimize the CO performance impact. Therefore, CO tolerant Ru-containing catalysts are generally used as anode catalysts in reformate-based PEMFCs [17,18]. Similarly, Ru-containing catalysts, such as Pt–Ru alloy and Pt–Ru metal oxides, are generally employed as anode catalysts for direct methanol fuel cells (DMFCs) due to their capabilities to remove adsorbed CO reaction intermediates that form during methanol electro-oxidation [19–21]. Even though more desirable performance can be achieved compared to Pt, the use of Ru-containing catalysts brings forth a major catalyst degradation

* Corresponding author. Tel.: +1 604 454 0900; fax: +1 604 412 4700.
E-mail address: tommy.cheng@ballard.com (T.T.H. Cheng).

0378-7753/$ – see front matter © 2010 Elsevier B.V. All rights reserved.
doi:10.1016/j.jpowsour.2010.02.028

mode, namely Ru crossover, which has been previously identified in DMFC in various studies [22–26]. The impacts of Ru contamination on oxygen-reduction reaction (ORR) kinetics have also been previously documented [22–25]. For instance, Gancs et al. has observed an 8-fold decrease in ORR kinetics with less than 20% Ru coverage [24]. Ru deposited on the cathode was also found to lower the ability of the cathode to tolerate methanol, which is known to crossover from the anode to the cathode in DMFCs [23]. However, Ru crossover in low-temperature hydrogen PEMFC, which can happen during PEMFC air/air start/stop, fuel starvation, or cell reversal operations, has not been documented as a critical catalyst degradation mechanism until a recent study [27]. In that study, Cheng et al. reported a 40% drop in ORR current at 0.9 V with 20% Ru coverage and in addition to the impact on cathode performance, a significant drop in CO tolerance was found with Ru degradation [27]. Hence, it is essential to study and gain better understanding of the stressors for Ru dissolution and subsequent crossover.

Depending on the quality and design of the reforming system, reformate fuel typically contains 10–50 ppm of CO, and up to 25% CO_2. Therefore, the hydrogen concentration in the anode may also vary, depending on the fuel re-circulation design. It is therefore important to understand the impacts of anode gas composition on catalyst degradation. In the present study, the effects of fuel gas composition on Ru dissolution and crossover were investigated in order to gain understanding of the Ru degradation mechanism.

2. Experimental

In the present investigation, the membrane-electrode assemblies (MEAs) were composed of carbon paper GDLs and full catalyst-coated membranes (CCMs) made with Pt-based cathode catalysts, anode catalysts containing Pt–Ru metal oxides, and perfluorinated sulfonic acid (Nafion®) membranes. Dynamic hydrogen electrodes (DHE) were incorporated into the MEAs to monitor the electrode voltages [28]. Additionally, an MEA without Ru was tested for reference.

The fuel cell experiments were carried out at 65 °C, 3 bar pressure, and 100% inlet relative humidity (RH) in a single-cell hardware with an active MEA area of 300 cm^2. An anode accelerated stress test (AST) was employed to cause Ru dissolution and crossover. Based on the measurements, the anode potential cycled typically 2000 times, between approximately 0 and 0.9 V vs. DHE during the AST, while the cathode potential was kept below 1.0 V to avoid carbon corrosion.

Cyclic voltammetric (CV) measurements of the cathode were performed periodically in-situ with a CorrWare software, using a PAR Model 263A potentiostat connected to a 20 A Kepco power booster. Hydrogen was fed to the anode and nitrogen on the cathode; therefore, the anode acted as a DHE. Before each CO stripping experiment, the cathode was cleaned electrochemically three times by cycling from 0.1 to 1.2 V vs. DHE at a scan rate of 20 mV s^{-1}. Subsequently, the cathode was poisoned with 1.0% CO gas balanced with nitrogen, followed by bulk CO purging with pure nitrogen. The CO stripping was then carried out by scanning between 0.1 and 1.2 V vs. DHE at a scan rate of 20 mV s^{-1}. After each CO stripping CV, a blank scan in nitrogen between 0.1 and 1.2 V vs. DHE was also recorded for background correction and double-layer charging current (DLCC) measurements. After CV experiments, the fuel cells were conditioned at the operational conditions described above for at least 30 min before polarization experiments.

In addition to in-situ electrochemical measurements, selected end-of-life (EOL) cathode catalysts were characterized by X-ray diffraction (XRD) and neutron activation analysis (NAA) to determine the catalyst particle size and composition, respectively. XRD spectra were acquired using a D8ADVANCE X-ray diffractometer

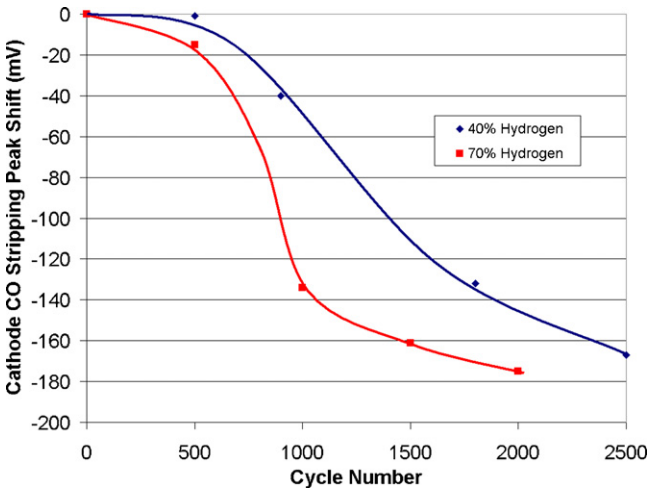

Fig. 1. Cathode CO stripping peak shift as a function of anode AST cycle number. AST performed under different hydrogen concentrations. Temperature: 65 °C; scan rate: 20 mV s^{-1}.

(Bruker Axs, Inc.) with a CuKα1 X-ray source scanning from 36 to 44° at an angle increment of 0.04°/step. NAA measurements were carried out by École Polytechnique using a SLOWPOKE nuclear reactor (Atomic Energy of Canada, Ltd.), and a germanium semiconductor gamma-ray detector (Ortec Model GEM55185).

3. Results and discussion

3.1. Effects of hydrogen concentration on anode degradation

Using the proprietary anode AST (see Section 2 for details), anode catalysts containing Pt–Ru metal oxides underwent potential cycling from 0 to 0.9 V vs. DHE under different gaseous environments, namely 40% hydrogen and 70% hydrogen, both balanced with nitrogen. The CV characteristic changes and performance impacts were monitored periodically throughout the tests.

It is known that Ru contamination on the cathode causes negative CO stripping peak shifts as the Ru promotes the electro-oxidation of CO [26,27,29,30]. It has also been reported that the presence of Ru causes an increase in DLCC due to the oxidation of elemental Ru to hydrous Ru oxides shown in Eq. (1) in the same potential region [31]:

$$Ru + 2H_2O \rightarrow Ru(OH)_2 + 2e^- + 2H^+ \quad (1)$$

After AST cycling, it is evident that the CO stripping peak potential shifted negatively due to Ru dissolution and crossover, and the cathode became more Pt–Ru-like. The CO stripping peak shift as a function of AST cycle number is shown in Fig. 1. It is clear that cycling in 70% hydrogen caused more negative CO stripping peak shifts as compared to cycling in 40% hydrogen, indicating that the degree of Ru crossover was more severe in the case of 70% hydrogen. The cathode DLCC also increased with AST cycling. Fig. 2 shows the % increases in cathode DLCC as a function of cycle number. In agreement with the relative level of CO stripping peak shifts, cycling in 70% hydrogen caused a greater increase in cathode DLCC than cycling in 40% hydrogen, concurring with the notion that cycling in 70% hydrogen led to a higher degree of Ru crossover.

In addition, the % performance losses at 1 A cm^{-2} are plotted against the AST cycle number in Fig. 3. The results agreed well with the relative severity of Ru crossover indicated by CV characteristic changes. Based on the experimental results, it is clear that Ru degradation is impacted by the hydrogen concentration in the fuel stream. It was previously reported by Hadzi-Jordanov et al. that Ru oxides formed at high anodic potentials could only

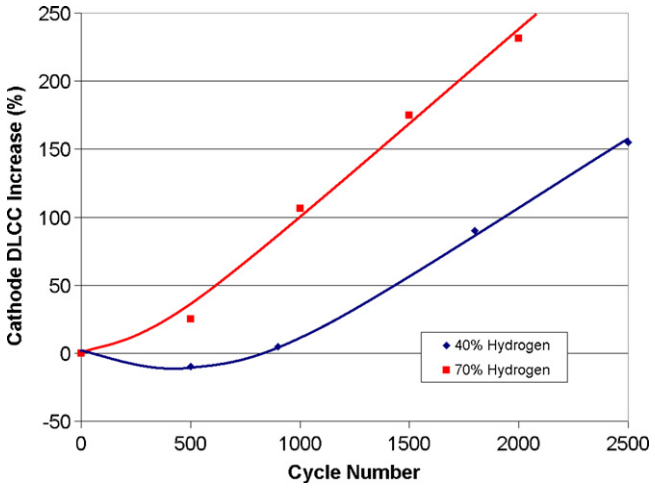

Fig. 2. % Increase in cathode DLCC at 0.45 V as a function of anode AST cycle number. AST performed under different hydrogen concentrations. Temperature: 65 °C; scan rate: 20 mV s^{-1}.

be reduced in the hydrogen evolution region with co-evolution of hydrogen [32]. Furthermore, it was suggested by Kotz and Stucki that RuO_2 could be partially reduced during H_2 evolution to Ru oxy-hydroxide possibly from hydrogen penetration [33]. Recently, it was also demonstrated that RuO_2 could be reduced to Ru in a 1% H_2/99% N_2 atmosphere at elevated temperature (150–250 °C) [34]. Therefore, it is believed that the Ru species present in our Pt–Ru metal oxide catalysts are first reduced to a more easily dissolved form, such as hydrous Ru oxides before leaching out and crossing over to the cathode.

3.2. Effects of carbon dioxide concentration on anode degradation

In addition to the study of the impacts of hydrogen concentration on Ru crossover, the effects of carbon dioxide concentration were also evaluated, as fuel produced from reformate-based fuel cell systems typically contains a significant fraction of carbon dioxide (20%). Again, using the above-mentioned proprietary anode AST, three different concentrations of carbon dioxide were fed into the anode: 0, 1, and 20 vol.%. The hydrogen concentration of the blends was kept between 70 and 72 vol.% and the remainder was balanced with nitrogen (see Table 1). It should also be noted that the potential cycling profiles (not shown) of the various tests were identical. Therefore, any differences observed in the experiments were not due to differences in cycling pattern, but rather the true effects from the compositions of the fuel blend.

Table 1
Anode AST gas compositions–effects of carbon dioxide concentration.

Test	H_2 (vol.%)	CO_2 (vol.%)	N_2 (vol.%)
1	70	0	30
2	72	1	27
3	72	20	8

The cathode CO stripping CVs of the fuel cells at the beginning-of-life (BOL) and after 500, 1000, 1500, and 2000 AST cycles are shown in Fig. 4. It is very evident that the CO stripping peak potential shifts were less apparent and essentially absent with the

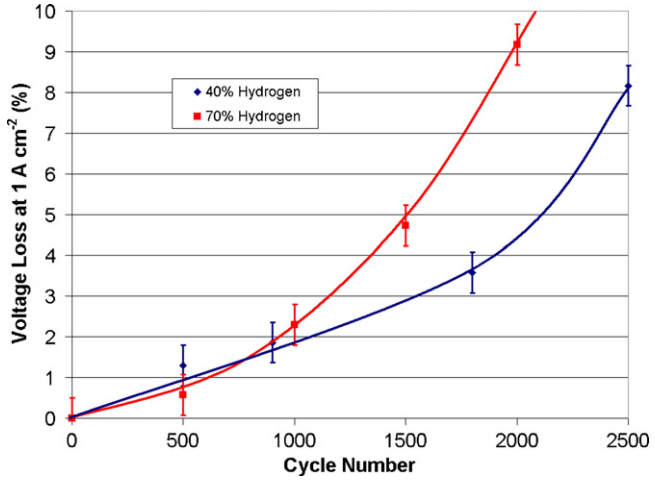

Fig. 3. % Performance loss as a function of anode AST cycle number. AST performed under different hydrogen concentrations.

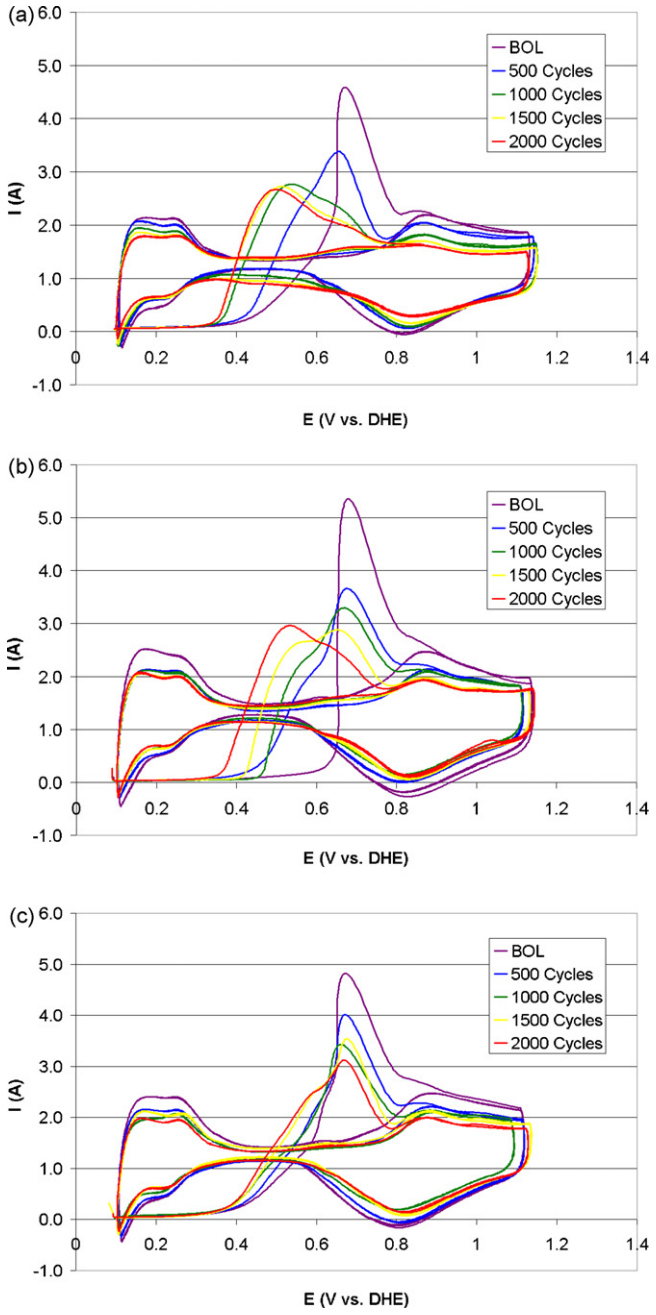

Fig. 4. Cathode CO stripping CVs–AST under different CO_2 concentrations. Temperature: 65 °C; scan rate: 20 mV s^{-1}. (a) 0% CO_2; (b) 1% CO_2; (c) 20% CO_2.

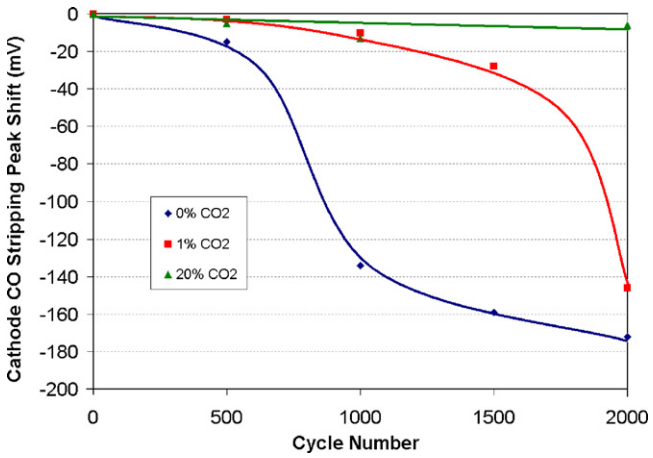

Fig. 5. Cathode CO stripping peak shift as a function of AST cycle number under different CO_2 concentrations. Temperature: 65 °C; scan rate: 20 mV s^{-1}.

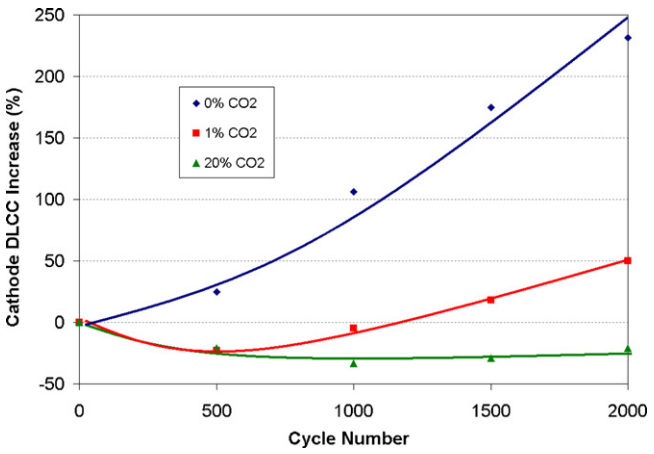

Fig. 7. % Increase in cathode DLCC as a function of AST cycle number under different CO_2 concentrations. Temperature: 65 °C; scan rate: 20 mV s^{-1}.

injection of 1 and 20 vol.% carbon dioxide, respectively. It should be pointed out that in the case of cycling with 20 vol.% carbon dioxide, the formation of an oxidation peak at approximately 0.6 V is associated with the changes in Pt surface structure and not due to Ru, as the same oxidation peak was observed in a Ru-free anode AST cycling experiment. In the case of injecting 1 vol.% carbon dioxide, the rate of CO stripping peak shift was approximately halved (i.e. the CO stripping peak potential shift after 2000 AST cycles with 1 vol.% carbon dioxide was similar to that after 1000 AST cycles without carbon dioxide) (see also Fig. 5). The results indicate that the Ru coverage on the cathode was lower when the AST was run in the presence of CO_2, suggesting that the presence of CO_2 could hinder Ru dissolution and crossover.

The relative changes in the cathode catalyst surface area determined by two different methods (CO stripping and hydrogen desorption) also supported the proposition. As shown in Fig. 6, the cathode surface area loss estimated by hydrogen desorption for the MEA cycled in the presence of 20 vol.% carbon dioxide was found to be the lowest, followed by 1 vol.% carbon dioxide, and lastly 0 vol.% carbon dioxide. Since Ru only provides minor contribution to the hydrogen adsorption/desorption charge, a higher degree of Ru contamination would result in a lower hydrogen adsorption/desorption charge, or a higher surface area loss by hydrogen desorption [24]. Hence, the observed order suggests that cycling without carbon dioxide led to the most severe Ru contamination among the different tests, agreeing well with the relative shifts in CO stripping peak potential.

Contrary to the relative order in surface area loss by hydrogen desorption, yet concurring with the above notion, the relative order in surface area loss by CO stripping displayed the opposite trend (i.e. cycling in the absence of carbon dioxide led to the lowest surface area loss by CO stripping). It is known in literature that Ru contamination causes an overestimation of catalyst surface area by CO stripping as the CO stripping charge incorporates contributions from other surface processes in the same potential range. It has been reported that up to 45% of the CO stripping charge was due to non-CO related surface processes [35]. Therefore, the order of Ru contamination suggested above was further supported by the observed trend for surface area loss by CO stripping.

The changes in cathode DLCC, which is highly indicative of Ru contamination, are shown in Fig. 7. Cycling without carbon dioxide injection resulted in the highest cathode DLCC increase while no increase was observed in the case of cycling in 20 vol.% carbon dioxide. Again, the results agreed well with the other CV characteristic changes.

The performance losses at 1 A cm^{-2} before and after the anode AST cycling are shown in Fig. 8. It is apparent that injecting carbon dioxide during AST cycling resulted in significantly lower performance losses, in agreement with the relative degree of Ru crossover. In the absence of carbon dioxide during the AST, 9% of voltage loss at 1 A cm^{-2} was observed after 2000 cycles. With the injection of 1 vol.% carbon dioxide during the AST cycling, the performance loss after 2000 cycles was reduced more than two-folds (3.3% volt-

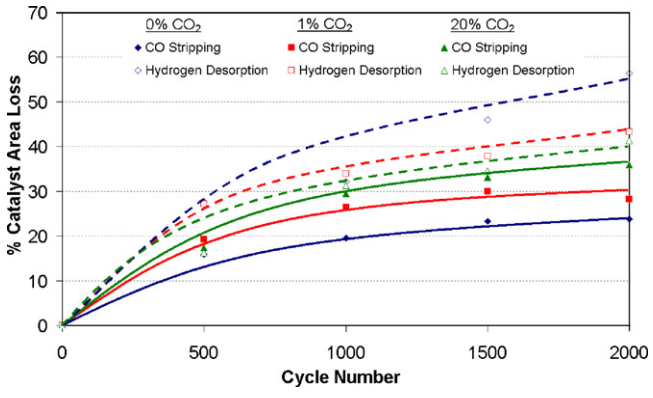

Fig. 6. % Catalyst area losses characterized by CO stripping and hydrogen desorption as a function of AST cycle number under different CO_2 concentrations. Temperature: 65 °C; scan rate: 20 mV s^{-1}.

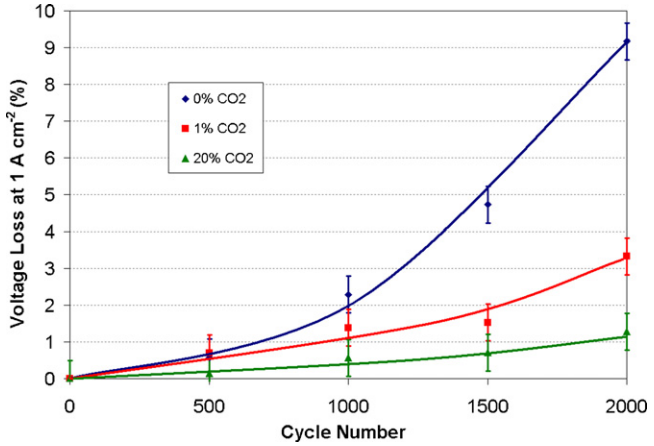

Fig. 8. % Performance loss as a function of anode AST cycle number. AST performed under different carbon dioxide concentrations.

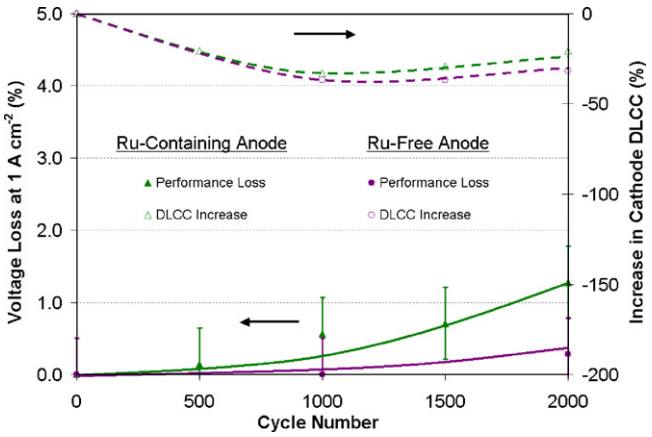

Fig. 9. % Performance loss and % increase in cathode DLCC as a function of anode AST cycle number. AST performed under 72% hydrogen, 20% carbon dioxide, and 8% nitrogen. For DLCC, scan rate: 20 mV s^{-1}.

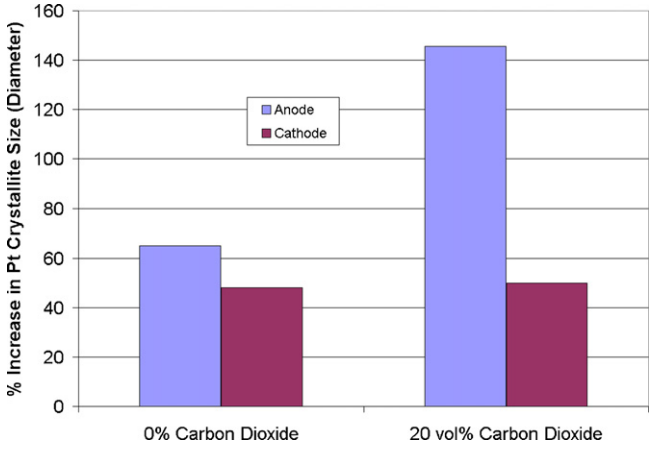

Fig. 11. % Increase in Pt crystallite size after 2000 anode AST cycles.

age loss). With 20 vol.% carbon dioxide, the performance loss was only minor (1.3% voltage loss after 2000 cycles). The results further signify the impact of Ru crossover on fuel cell performance and durability. Additionally, a Ru-free MEA was cycled using the anode AST for comparison. As shown in Fig. 9, the Ru-containing MEA cycled in 20 vol.% carbon dioxide showed essentially identical performance losses and CV characteristic changes as the Ru-free MEA, further supporting that cycling in 20 vol.% carbon dioxide resulted in very little to no Ru crossover.

Fig. 10 shows the Ru concentration in the cathode catalyst layers, measured by NAA, after 2000 anode AST cycles. Based on the data, it is now confirmed that cycling in 20 vol.% carbon dioxide yielded more than a 10-fold reduction in Ru contamination on the cathode. However, injecting carbon dioxide led to more severe anode catalyst agglomeration (see Fig. 11). The catalyst crystallite sizes were determined by XRD using Scherrer's formula (Eq. (2)). The results indicate that Pt agglomeration on the anode became more preferable in the presence of carbon dioxide as Ru dissolution was suppressed. In contrast, there was no difference in cathode catalyst crystallite size increase between cycling with and without carbon dioxide during the anode AST.

$$d = \frac{0.9\lambda}{B\cos\theta} \quad (2)$$

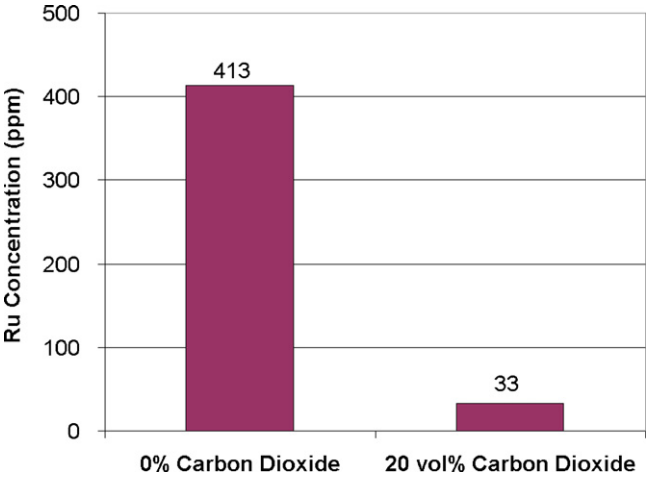

Fig. 10. Ru concentration in the cathode catalyst layers by NAA after 2000 anode AST cycles.

3.3. Ru dissolution mechanism from Pt–Ru metal oxides

From the experimental results (both hydrogen and carbon dioxide concentration effects), it is evident that hydrogen and carbon dioxide can, respectively accelerate and hinder the dissolution of Ru. It was hypothesized in Section 3.1 that the Ru species in our Pt–Ru metal oxide catalysts need to be reduced to a more unstable state before dissolving and crossing over to the cathode. In conjunction with the fact that carbon dioxide impedes Ru dissolution, it is reasonable to believe that carbon dioxide can possibly inhibit the hydrogen–Ru interaction by adsorbing onto the Ru oxide surface at low potential regions, thereby prohibiting the reduction of Ru oxides and subsequent Ru dissolution. It is known that there is strong interaction between carbon dioxide and transition metal/metal oxides, including Ru oxides [36,37], in ultra-high vacuum conditions however, it must be noted that there is no published relevant study on carbon dioxide–Ru interaction under fuel cell conditions. It is also possible that carbon dioxide may use up some free energy during its desorption in the potential cycling at high potentials, so less energy is available to degrade the Ru anode. Furthermore, water management may be affected favourably due to the dissolution of carbon dioxide in water. Carbon monoxide, which may be produced from the reverse water gas-shift reaction, may also take part in the Ru degradation inhibition mechanism. More studies are required to better understand the carbon dioxide effect.

4. Conclusions

An anode AST was employed to study the effects of gas compositions during anode potential cycling on Ru dissolution and crossover. Based on the performance losses and the changes in cathode CV characteristics, such as the CO stripping peak potential and DLCC, it was found that hydrogen accelerated the dissolution of Ru and hence led to more severe Ru crossover. In contrast, the presence of carbon dioxide hindered the degradation of Ru, as confirmed by NAA results, CV characteristic changes, and the relative performance losses. In particular, the injection of 20 vol.% carbon dioxide yielded very minor Ru crossover, which displayed essentially identical trends as the Ru-free MEA after cycling. It was hypothesized that the presence of carbon dioxide limited the Ru–hydrogen interactions and inhibited possibly a preceding Ru reduction step required for dissolution. It was also found that anode Pt agglomeration became more severe and caused bigger increases in catalyst size as Ru dissolution was suppressed. The results pro-

vided mechanistic understanding of Ru dissolution and highlighted the importance of preventing Ru crossover.

Acknowledgements

The authors thank the University of British Columbia Department of Chemistry for XRD and École Polytechnique for NAA.

References

[1] D. Papageorgopoulos, "Fuel Cell Technologies", US DOE Merit Review, 2009.
[2] M.S. Wilson, F.H. Garzon, K.E. Sickafus, S. Gottesfeld, J. Electrochem. Soc. 140 (1993) 2872.
[3] S.D. Knights, K.M. Colbow, J. St-Pierre, D.P. Wilkinson, J. Power Sources 127 (2004) 127.
[4] S. Stucki, G.G. Scherer, S. Schlagowski, E. Fischer, J. Appl. Electrochem. 28 (1998) 1041.
[5] R.M. Darling, J.P. Meyers, J. Electrochem. Soc. 150 (2003) A1523.
[6] M. Laporta, M. Pegoraro, L. Zanderighi, Phys. Chem. Chem. Phys. 1 (1999) 4619.
[7] R. Borup, J. Meyers, B. Pivovar, Y.S. Kim, R. Mukundan, N. Garland, D. Myers, M. Wilson, F. Garzon, D. Wood, P. Zelenay, K. More, K. Stroh, T. Zawodzinski, J. Boncella, J.E. McGrath, M. Inaba, K. Miyatake, M. Hori, K. Ota, Z. Ogumi, S. Miyata, A. Nishikata, Z. Siroma, Y. Uchimoto, K. Yasuda, K.I. Kimijima, N. Iwashita, Chem. Rev. 107 (2007) 3904.
[8] A.S. Arico, A. Stassi, E. Modica, R. Ornelas, I. Gatto, E. Passalacqua, V. Antonucci, J. Power Sources 178 (2008) 525.
[9] Y. Shao-Horn, W.C. Sheng, S. Chen, P.J. Ferreira, E.F. Holby, D. Morgan, Top. Catal. 46 (2007) 285.
[10] J. Xie, D.L. wood, D.M. Wayne, T.A. Zawodzinski, P. Atanassov, R.L. Borup, J. Electrochem. Soc. 152 (2005) A104.
[11] D.C. Papageorgopoulos, F.A. de Bruijn, J. Electrochem. Soc. 149 (2002) A140.
[12] J.M. Moore, P.L. Adcock, J.B. Lakeman, G.O. Mepsted, J. Power Sources 85 (2000) 254.
[13] R. Mohtadi, W.K. Lee, J.W. Van Zee, J. Power Sources 138 (2004) 216.
[14] R. Halseid, P.J.S. Vie, R. Tunold, J. Power Sources 154 (2006) 343.
[15] H.J. Soto, W.L. Lee, J.W. Van Zee, M. Murthy, Electrochem. Solid-State Lett. 6 (2003) A133.
[16] M. Inaba, M. Sugishita, J. Wada, K. Matsuzawa, H. Yamada, A. Tasaka, J. Power Sources 178 (2008) 699.
[17] A.S. Arico, S. Srinivasan, V. Antonucci, Fuel Cells 1 (2001) 133.
[18] K. Koczkur, Q.F. Yi, A.C. Chen, Adv. Mater. 19 (2007) 2648.
[19] Z.G. Shao, F. Zhu, W.F. Lin, P.A. Christensen, H. Zhang, J. Power Sources 161 (2006) 813.
[20] K. Lasch, L. Jorissen, J. Garche, J. Power Sources 84 (1999) 225.
[21] H.B. Suffredini, V. Tricol, N. Vatistas, L.A. Avaca, J. Power Sources 158 (2006) 124.
[22] P. Peila, C. Eickes, E. Brosha, F. Garzon, P. Zelenay, J. Electrochem. Soc. 151 (2004) A2053.
[23] G.S. Park, C. Pak, Y.S. Chung, J.R. Kim, W.S. Jeon, Y.H. Lee, K. Kim, H. Chang, D. Seung, J. Power Sources 176 (2008) 484.
[24] L. Gancs, B.N. Hult, N. Hakim, S. Mukerjee, Electrochem. Solid-State Lett. 10 (2007) B150.
[25] L. Gancs, N. Hakim, B.N. Hult, S. Mukerjee, ECS Trans. 3 (2006) 607.
[26] J.H. Choi, Y.S. Kim, R. Bashyam, P. Zelenay, ECS Trans. 1 (2006) 437.
[27] T. Cheng, V. Colbow, S. Wessel, 217th ECS Meeting, Vancouver, April 2010.
[28] M.V. Lauritzen, P. He, A.P. Young, S. Knights, V. Colbow, P. Beattie, J. New Mater. Electrochem. Syst. 10 (2007) 143.
[29] H.A. Gasteiger, N. Markovic, P.N. Ross, E.J. Cairns, J. Phys. Chem. 98 (1994) 617.
[30] H.N. Dinh, X. Ren, F.H. Garzon, P. Zelenay, S. Gottesfeld, J. Electroanal. Chem. 491 (2000) 222.
[31] T. Frelink, W. Visscher, J.A.R. vanVeen, Langmuir 12 (1996) 3702.
[32] S. Hadzi-Jordanov, H. Angerstein-Kozlowska, M. Vukovic, B.E. Conway, J. Electrochem. Soc. 125 (1978) 1471.
[33] E.R. Kotz, S. Stucki, J. Appl. Electrochem. 17 (1987) 1190.
[34] E.V. Jelenkovic, K.Y. Tong, W.Y. Cheung, S.P. Wong, Microelectron. Reliab. 43 (2003) 49.
[35] T. Nagel, N. Bogolowski, H. Baltruschat, J. Appl. Electrochem. 36 (2006) 1297.
[36] H.J. Freund, M.W. Roberts, Surf. Sci. Rep. 25 (1996) 225.
[37] Y. Wang, A. Lafosse, K. Jacobi, J. Phys. Chem. B 106 (2002) 5476.